Photomagnetic Nanocomposites

Transparent, Superparamagnetic $K_x^I Co_y^{II}[Fe^{III}(CN)_6]$–Silica Nanocomposites with Tunable Photomagnetism

*Joshua G. Moore, Eric J. Lochner, Chris Ramsey, Naresh S. Dalal, and A. E. Stiegman**

There has been considerable interest in molecular magnets based on the Prussian blue class of transition-metal cyanide complexes.[1] Pioneering work on these materials has realized a broad range of ferro- and ferrimagnetic solids with Curie points ranging from cryogenic to above room temperature.[2,3] A parallel interest also exists in the development of nanocomposite structures containing nanoscale magnetic particles exhibiting single-domain magnetic behavior.[4–6] Investigations of magnetic nanocomposites is driven by their novel properties and their potential as new magnetic, optical, and electronic materials. With one exception,[7] however, the Prussian blue class of magnetic materials has not been produced as nanoparticles, and, to the best of our knowledge, there have been no reports of their incorporation into composite structures. Herein we report the fabrication of a new nanocomposite material containing $K_xCo_y^{II}[Fe^{III}(CN)_6]_z$, a ferromagnetic analogue of Prussian blue, in a porous silica matrix. This material is made by a controlled multicomponent sol–gel synthesis in which the precipitation of the Prussian blue analogue is arrested at nanoscale dimensions by gelation of the silica network. The resulting materials are homogeneous, optically transparent, and exhibit superparamagnetic and tunable photomagnetic behavior. We believe that this study suggests a new approach for utilizing the Prussian blue class of magnetic materials in advanced optical and magnetic applications.

Homogeneous silica xerogels containing cyanide-bridged Co^{II}/Fe^{III} centers were made by incorporation of both transition-metal components during the solution phase of the synthesis. To obtain homogeneous materials reproducibly, conditions were optimized for the amount of water and the concentration and molar ratio of Co^{II} and ferricyanide by following previously developed procedures.[8,9] In the optimized preparation, Co^{II} nitrate was dissolved in methanol and added to tetramethylorthosilicate. Aqueous potassium ferricyanide was added to this solution to give a 1:1 Co:Fe molar ratio. Upon mixing, the solution turns dark purple, which suggests the formation of the mixed-valence complex. At concentrations up to 0.03 mol % total-metal to silicon (Fe + Co/Si), the solution remained transparent through gelation, aging, and drying, and ultimately yielded a homogeneous, optically transparent xerogel (Figure 1, inset). The spectrum of this glass (Figure 1) is qualitatively similar to that of the bulk materials, with a broad intervalence charge-transfer band in the visible region between 450 and 650 nm and a sharp, higher energy peak around 400 nm. However, the maximum of the intervalence band lies at 452 nm

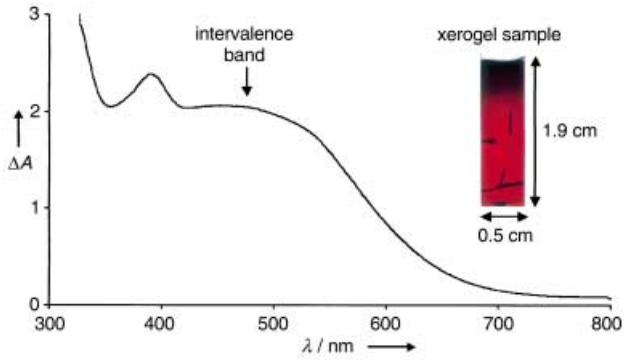

Figure 1. The optical absorption spectrum of a 0.03 mol % Co^{II}/Fe^{III} xerogel (inset) shows an intervalence charge-transfer band in the range 450–650 nm with a maximum at 452 nm.

(22 124 cm^{-1}) which is blue-shifted by approximately 2900 cm^{-1} from that of the bulk materials. To determine whether the magnetic behavior was singular, the magnetic susceptibility of these materials was measured as a function of temperature and field strength.[10] Bulk $M_x^I Co_y^{II}[Fe^{III}(CN)_6]_z$ (M^I = alkali-metal cation) shows ferromagnetic behavior in its field-cooled (FC) magnetization, with a Curie temperature of 14.0 K.[11,12] However, this complex, along with other first-row Prussian blue analogues, also shows blocking behavior in the zero-field-cooled (ZFC) magnetization, which has been attributed to spin-glass properties arising from defects in the lattice.[13,14] While it might be expected that a dilute dispersion of $K_xCo_y^{II}[Fe^{III}(CN)_6]_z$ in a xerogel would exhibit only simple paramagnetic behavior, the FC and ZFC magnetization as a function of temperature for a 0.03 mol % Co^{II}/Fe^{III} xerogel (Figure 2a) indicates more complex behavior. The FC magnetization parallels that of the bulk complex above 5 K but has a lower Curie temperature ($T_c \approx 13$ K). The ZFC magnetization curve shows a well-defined peak at 10 K. Above this temperature, the FC and ZFC magnetization curves converge and become coincident. This magnetization behavior is characteristic of blocking in a superparamagnetic system of small, single-domain particles or, as it is in the bulk, the glass transition in a spin glass.[15] Measurement of the magnetization as a function of field strength at 5 K, below the blocking temperature (Figure 2b), reveals hysteretic behavior that reaches a magnitude of 7.08×10^3 emu mol^{-1} at 5 kOe with a coercive field of approximately 0.41 kOe. From room temperature down to the blocking temperature (10 K) no hysteresis is observed (Figure 2c). These observations are also consistent with both spin-glass and superparamagnetism. However, the hysteresis loops measured under FC and ZFC conditions at 5 K are identical and symmetric about the center; this is one of the defining characteristics of super-

[*] Prof. A. E. Stiegman, J. G. Moore, C. Ramsey, Prof. N. S. Dalal
The Department of Chemistry and Biochemistry
Florida State University
Tallahassee, FL 32306 (USA)
Fax: (+1) 850-644-6605
E-mail: stiegman@chem.fsu.edu
E. J. Lochner
Materials Research and Technology Center (MARTECH)
Florida State University
Tallahassee, FL 32306 (USA)

 DOI: 10.1002/ange.200250409

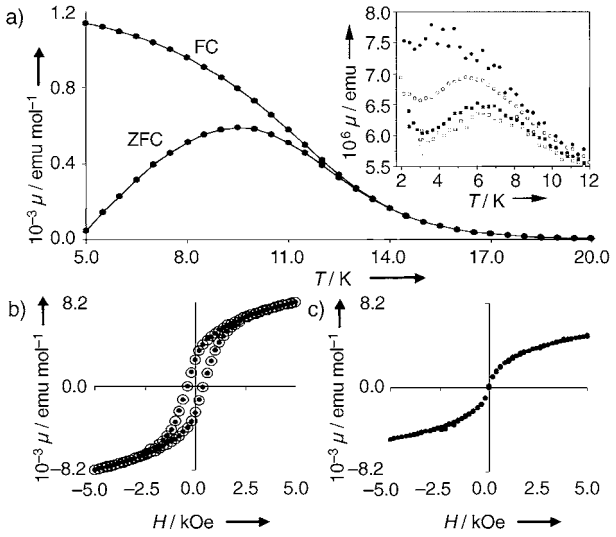

Figure 2. a) Field-cooled (FC) and zero-field-cooled (ZFC) dc magnetization versus temperature curves at $H = 100$ Oe [inset: frequency dependence of ac susceptibility: 100 (●), 1000 (○), 5000 (■), and 10000 Hz (□)]. b) FC (●) and ZFC (○) hysteresis loops at $T = 5$ K. c) Hysteresis loop at $T = 13$ K.

paramagnetism and suggests that this property, possibly superimposed by the inherent spin-glass properties of the bulk, is present in these materials.[15,16] This conclusion is also consistent with ac susceptibility data (Figure 2, inset), which show a significant frequency-dependent, thermally activated magnetization reversal dynamics with an activation energy of 29 ± 1 K ($160\,\mathrm{J\,mol^{-1}}$) and $\tau_0 = 3 \times 10^{-6}$ s. This frequency dependence is a unique property of these materials and is significantly different from that of the bulk, as frequency dependence has not been observed in this composition.

Support for a superparamagnetic origin of the magnetic properties and an explanation of the blue shift in the absorption spectrum is provided by the observation of $K^{I}_{x}Co^{II}_{y}[Fe^{III}(CN)_6]_z$ nanoparticles in the silica matrix. These particles can be observed directly by transmission electron microscopy, which reveals small domains, approximately 8–10 nm in size, distributed in the amorphous matrix (Figure 3). The strong diffraction of these domains verifies that they are crystalline, and quantitative analysis of the electron diffraction pattern (Figure 3, inset) yields d spacings identical to those of bulk $Co^{II}_{3}[Fe^{III}(CN)_6]_2$, and hence they can be unambiguously assigned to the mixed-valence compound. Since the synthesis of these materials is carried out by mixing solutions of the various components to form a homogeneous sol–gel solution, the formation of nanoparticles must occur spontaneously during some phase of the process. Given the large formation constants for Prussian blue analogues, the existence of nanoparticles in the matrix (as opposed to bulk phase-separated regions) strongly suggest that gelation of the silica effectively arrests the precipitation of $K^{I}_{x}Co^{II}_{y}[Fe^{III}(CN)_6]_z$ and sequesters the particles. We believe this to be the first time that nanoparticles of this type of materials have been generated in this way.

Among the most interesting properties of bulk $C^{I}_{x}Co^{II}_{y}[Fe^{III}(CN)_6]_z$ is its photomagnetism, which was first

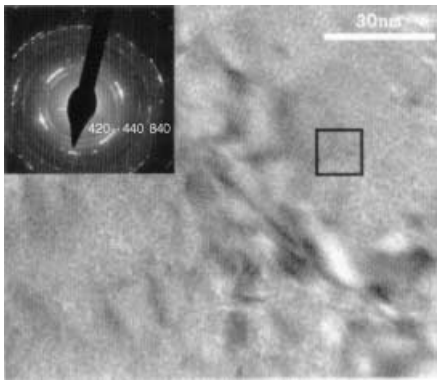

Figure 3. TEM image of a powdered Co^{II}/Fe^{III} xerogel showing nanoparticle crystalline structures with a size of 8–10 nm (inset: indexed diffraction pattern of the nanoparticles shown).

reported by Hashimoto.[12] Specifically, incidence of red light ($\lambda \approx 600$ nm) at temperatures below 150 K results in a net increase in the magnetization of the bulk material. This increase in magnetization can be erased by heating or irradiation with higher energy light ($\lambda \approx 450$ nm). As shown in Figure 4a, an analogous photomagnetic effect is observed in the nanocomposite system: irradiation of the glass ($\lambda \geq 550$ nm) results in an increase in magnetization, which, on returning to thermal equilibrium after the radiation source is extinguished, amounts to 7.6%. As with the bulk material, this magnetization could be decreased by irradiation with blue light ($\lambda = 448$ nm). Photomagnetic behavior in these materials arises from the presence of diamagnetic Co^{III}/Fe^{II} impurity sites in the $C^{I}_{x}Co^{II}_{y}[Fe^{III}(CN)_6]_z$ lattice. Absorption of light by these impurities at low temperature results in electron transfer to create a paramagnetic Co^{II}/Fe^{III} metastable state that increases the magnetization of the bulk.[12] Detailed studies of the system indicated that, on increasing the ligand-field strength around the Co^{II} centers, electron transfer from cobalt to iron occurs and generates more Co^{III}/Fe^{II} defect sites. These additional defect sites increase the magnitude of the photomagnetic effect.[17–19] In the bulk materials modification of the ligand field around cobalt is accomplished by the addition of alkali-metal cations, which change the stoichiometry of the complex and increase the degree of nitrogen coordination around the metal centers.[17,20] We found that, because of the porous nature of the silica matrix, direct substitution of the cobalt centers by ammine and other higher field ligands can be accomplished cleanly and in a highly controlled fashion. As shown in Figure 4b, passing ammonia over the composite results in continuous spectral changes that are highly isosbestic. The broad intervalence charge-transfer band is replaced by a single peak (470 nm) characteristic of hexammine Co^{III} centers, which suggests that diamagnetic defect sites have been created. Measurement of the magnetization of the composite as a function of ammine doping shows a steady decrease in magnetization, and the materials become diamagnetic at the highest levels of doping. Changes in the magnitude of the photomagnetic effect as a function of exposure to ammonia are shown in Figure 4c. With small exposure increments the magnetization increases until a maximum is reached at about 9.4% above that of the doped

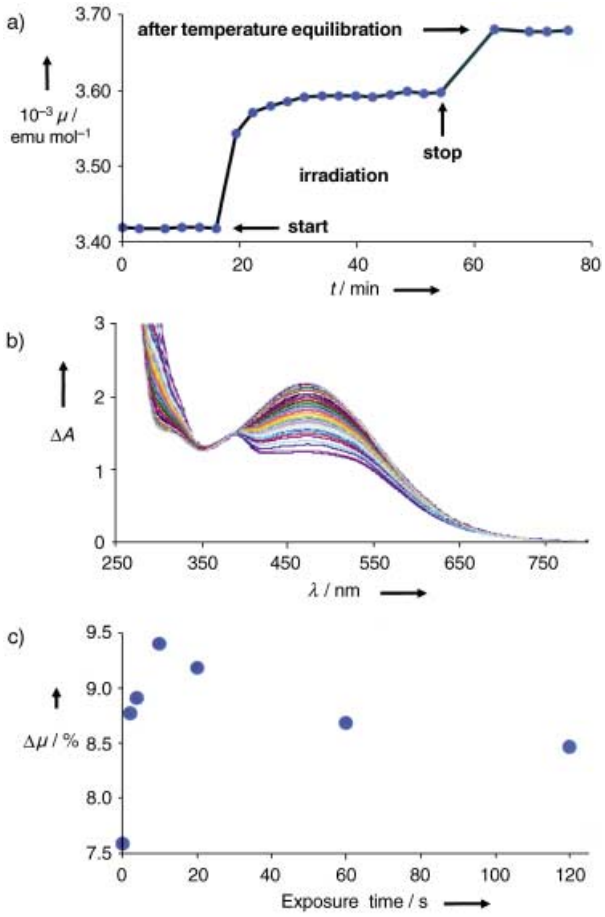

Figure 4. a) Photomagnetic effect at $\lambda \geq 550$ nm, $H = 500$ Oe, and $T = 5$ K. b) A series of optical absorption spectra taken every 30 min while anhydrous ammonia flowed over a 0.03 mol% Co^{II}/Fe^{III} xerogel. c) Percentage increase in magnetization of NH_3-substituted xerogels as a function of NH_3 exposure time (10 μL dose).

but nonirradiated composite. Above this threshold the photomagnetic effect decreases, and at high degrees of substitution the effect vanishes. This change is consistent with observations on the bulk material, which show that large numbers of the diamagnetic Co^{III}/Fe^{II} defect sites result in significantly diminished photomagnetism. In the bulk material this has been explained as arising from an increased rigidity in the lattice as the number of Co^{III}/Fe^{II} sites increases. This rigidity can no longer accommodate the bond-length increases that accompany the electron transfer of the Co^{II}/Fe^{III} sites to the metastable state.[17], Although such a rigidity effect may also be acting in the nanocrystals, high degrees of ammine substitution may ultimately result in disruption of the CN bridge with concomitant deactivation of the electron-transfer pathway, which would also degrade the effect.

Experimental Section

The 0.03% Co^{II}/Fe^{III} xerogel was made in the following manner: a solution of H_2O (4.6 mL), methanol (20.8 mL), and an aqueous solution of $K_3[Fe(CN)_6]$ (2.2 mM; 13.9 mL) was added dropwise to a solution containing tetramethylorthosilicate (30.3 mL), methanol (16.4 mL), and $Co(NO_3)_2$ (2.2 mM; 13.9 mL) in methanol, which gives an overall concentration of 0.31 mM for each metal. Then 4 mL of solution was placed into polystyrene cuvettes for gelation, aging, and drying phases. After gelation the xerogel has 12% of the original volume with a final concentration of each metal of approximately 3 mM.

Received: October 22, 2002 [Z50409]

Keywords: cobalt · iron · magnetic properties · nanostructures · sol–gel processes

[1] K. R. Dunbar, R. A. Heintz in *Progress in Inorganic Chemistry, Vol 45*, John Wiley & Sons, New York, **1997**, p. 283.
[2] S. Ferlay, T. Mallah, R. Ouahes, P. Veillet, M. Verdaguer, *Nature* **1995**, *378*, 701.
[3] W. R. Entley, G. S. Girolami, *Science* **1995**, *268*, 397.
[4] E. Cattaruzza, F. Gonella, G. Mattei, P. Mazzoldi, D. Gatteschi, C. Sangregorio, M. Falconieri, G. Salvetti, G. Battaglin, *Appl. Phys. Lett.* **1998**, *73*, 1176.
[5] I. S. Edelman, R. Ivantsov, A. Vasiliev, S. Stepanov, E. Kornilova, T. Zarubina, *Physica B* **2001**, *301*, 203.
[6] B. H. Sohn, R. E. Cohen, *Chem. Mat.* **1997**, *9*, 264.
[7] S. Vaucher, J. Fielden, M. Li, E. Dujardin, S. Mann, *Nano Lett.* **2002**, *2*, 225.
[8] M. D. Curran, T. E. Gedris, A. E. Stiegman, G. A. Plett, *Chem. Mat.* **1999**, *11*, 1120.
[9] M. D. Curran, D. D. Poore, A. E. Stiegman, *Chem. Mat.* **1998**, *10*, 3156.
[10] dc magnetic measurements were made with a superconducting quantum interference device (SQUID; Quantum Design MPMS XL-7). ac measurements were made on a Quantum Design PPMS.
[11] S. Juszczyk, C. Johansson, M. Hanson, A. Ratuszna, G. Malecki, *J. Phys. Condens. Matter* **1994**, *6*, 5697.
[12] O. Sato, T. Iyoda, A. Fujishima, K. Hashimoto, *Science* **1996**, *272*, 704.
[13] W. E. Buschmann, J. S. Miller, *Inorg. Chem.* **2000**, *39*, 2411.
[14] D. A. Pejakovic, J. L. Manson, J. S. Miller, A. J. Epstein, *Synth. Met.* **2001**, *122*, 529.
[15] J. K. Vassiliou, V. Mehrotra, M. W. Russell, E. P. Giannelis, R. D. McMichael, R. D. Shull, R. F. Ziolo, *J. Appl. Phys.* **1993**, *73*, 5109.
[16] J. L. Garcia, A. Lopez, F. J. Lazaro, C. Martinez, A. Corma, *J. Magn. Magn. Mater.* **1996**, *158*, 272.
[17] A. Bleuzen, C. Lomenech, V. Escax, F. Villain, F. Varret, C. C. D. Moulin, M. Verdaguer, *J. Am. Chem. Soc.* **2000**, *122*, 6648.
[18] C. C. D. Moulin, F. Villain, A. Bleuzen, M. A. Arrio, P. Sainctavit, C. Lomenech, V. Escax, F. Baudelet, E. Dartyge, J. J. Gallet, M. Verdaguer, *J. Am. Chem. Soc.* **2000**, *122*, 6653.
[19] V. Escax, A. Bleuzen, C. C. D. Moulin, F. Villain, A. Goujon, F. Varret, M. Verdaguer, *J. Am. Chem. Soc.* **2001**, *123*, 12536.
[20] The magnetic properties of this and other Prussian blue analogues are dependent on the exact composition of the complex, including the amount of alkali-metal present in the lattice. In the case of the nanocomposite materials reported here, the total amount of metals is so low that an accurate determination of the amount of K^+ ions present in the lattice of the nanoparticles (as opposed to the gross quantity present in the material as a whole) proved impossible by conventional techniques. Bulk $K^I_xCo^{II}_y[Fe^{III}(CN)_6]_z$ made under the same conditions of stoichiometry and concentrations was found, from X-ray fluorescence and FTIR measurements, to have the formula $K_{0.27}Co^{II}_{1.33}[Fe^{III}(CN)_6]$, which is close to that of the materials studied by Sato et al.[12], but we cannot assert that this composition is retained in the nanoparticles.

